Kinetic Analysis of Thermal Decomposition Process of Emulsion Explosive Matrix in the Presence of Sulfide Ores

Yang, Fuqiang; Guo, Yong; Lai, Yong; Hong, Yidu; Yuan, Shuaiqi

DOI
10.3390/su141811614

Publication date
2022

Document Version
Final published version

Published in
Sustainability (Switzerland)

sustainability

MDPI

Article

Kinetic Analysis of Thermal Decomposition Process of Emulsion Explosive Matrix in the Presence of Sulfide Ores

Fuqiang Yang [1], Yong Guo [1], Yong Lai [1], Yidu Hong [1,*] and Shuaiqi Yuan [2,*]

[1] College of Environment and Safety Engineering, Fuzhou University, Fuzhou 350116, China
[2] Safety and Security Science Group, Faculty of Technology, Policy and Management, TU Delft, 2628 BX Delft, The Netherlands
* Correspondence: yidu.hong@fzu.edu.cn (Y.H.); s.yuan-2@tudelft.nl (S.Y.)

Abstract: This study aims to characterize the whole reaction process of (i) emulsion explosive matrix and sulfide ores, and (ii) ammonium nitrate and pyrite by the thermodynamics analysis method. A series of experiments were carried out at atmospheric pressure from 25 °C to 350 °C at four heating rates (3, 5, 10, and 15 K/min) and the Coats–Redfern method was applied to calculate the apparent activation energy of samples at different heating rates. The results show that the thermogravimetric (TG) curve of sulfide ores and emulsion explosive matrix can be divided into four stages: the water evaporation stage, the dynamic balance stage, the thermal decomposition stage, and the extinguishment stage. However, the thermal decomposition process of ammonium nitrate and pyrite can be divided into the dynamic balance stage, the thermal decomposition stage, and the burnout stage. The ignition temperature (T_0) and maximum peak temperature (T_m) of the samples increased with the heating rate, but the shape of the TG/DTG (Derivative Thermogravimetric) curve was not affected. The results show that the reaction process of sulfide ores and emulsion explosive matrix is similar to the reaction process of pyrite and ammonium nitrate. The thermal stability of emulsion explosive matrix decreases when sulfide ores are added. By contrast, when pyrite is added, the thermal stability of the ammonium nitrate decreases more significantly.

Keywords: sulfide ores; emulsion explosive matrix; activation energy; self-denotation; thermodynamics analysis

Citation: Yang, F.; Guo, Y.; Lai, Y.; Hong, Y.; Yuan, S. Kinetic Analysis of Thermal Decomposition Process of Emulsion Explosive Matrix in the Presence of Sulfide Ores. *Sustainability* **2022**, *14*, 11614. https://doi.org/10.3390/su141811614

Academic Editors: Chaolin Zhang, Shoujian Peng, Bobo Li and Gerardo Maria Mauro

Received: 25 July 2022
Accepted: 13 September 2022
Published: 15 September 2022

1. Introduction

Sulfide ores include various sulfide minerals that are essential raw chemical materials for promoting the development of the chemical process industries and agriculture in China [1]. As a type of industrial explosive, the emulsion explosive (EE) is widely used during the mining process for sulfide ores. Sulfide ores may be oxidized with oxygen and water and thus release a large amount of heat, which may result in heat accumulation and temperature rising in blast holes. This may induce the premature detonation of EE. Moreover, the mineral consumption of China has increased dramatically and mining depth increases annually to meet the needs of spectacular economic growth [2]. At the same time, deep mining inevitably brings a series of problems to the mining process, such as in situ stress increasing and the temperature rising, which risk the self-detonation of EE. In the past few decades, several spontaneous explosion accidents have happened in high-sulfur mines all over the world, such as the Meikle gold mine in the USA, Mt Con Gold Mine in Canada [3], Dongxiang Copper Mine and Yunfu Pyrite in China. While the risk of fires (and, hence, significant damage) can be mitigated by leaching, the use of explosives is another factor that can increase fire risk, due to reactions between the ores and EE [4]. Therefore, a systemic understanding of the reaction between sulfide ores and emulsion explosives/emulsion explosive matrix is essential for preventing, controlling, and mitigating fire and explosion risks.

Gunawan and others investigated the reaction between ammonium nitrate (AN) and pyrite at the heating rate of 10 °C/min by Thermogravimetric (TG) analysis and differential scanning calorimetry (DSC) [5]. Priyananda and others found that the self-detonation of EE is closely related to the formation and aggregation of NO bubbles by using a video microscope [6]. Nakamura and others concluded that the exothermic reaction of AN and pyrite occurs at 190 °C, affected by the composition of experimental samples and the environment [7]. Xu and others analyzed the thermal decomposition process of EE and pyrite using TG-DSC and mass spectrometry (MS) [8]. The results indicate that pyrite can reduce the decomposition temperature of AN and EE and accelerate their decomposition rates. Liu and others used TG-DSC to test the non-isothermal thermal decomposition process of EE in nitrogen and an air atmosphere and also calculated its thermal kinetic parameters by various methods [9]. Djerdjev and others detected the gas production of AN and pyrite heated to 55 °C by using an infrared spectrometer [10]. Vázquez calculated the kinetic parameters of the oxidative reactions of pyrite with different methods [11]. Ruan studied the decomposition process of pyrite by SEM-EDS analysis. The activation energies of pyrite in the two decomposition steps were 297.86 kJ/mol and 249.30 kJ/mol. In addition, the relationship between kinetic parameters and temperature was determined [12]. Yang and others analyzed the thermal behaviors and apparent activation energies of sulfide ore samples at different heating rates before and after pre-oxidation. They concluded that apparent activation energy decreases from 364.017 to 474.228 kJ/mol, to 244.523 to 333.161 kJ/mol after pre-oxidation [13]. However, the samples used in the above studies only considered pure ammonium nitrate and pyrite. The thermal reaction kinetics of a single component cannot reveal the actual reaction between sulfide ores and emulsion explosives. Therefore, the influence of other sulfide minerals and ammonium nitrate on emulsion explosives needs further investigation.

In this study, thermogravimetric analysis was employed to characterize the reaction process of sulfide ores and emulsion explosive matrix, and pyrite and ammonium nitrate at different heating rates. Due to safety concerns, sensitized emulsion explosives were not investigated in the experiments. Meanwhile, the thermodynamic analysis method of Coats–Redfern was conducted to explore the reaction mechanism and calculate the activation energy of the samples. This paper aims to reveal the thermal decomposition characteristics of emulsion explosive matrix in the presence of sulfide ores and provide a reference for the prevention and control of explosive accidents in high-sulfur mines.

2. Materials and Methods

2.1. Sulfide Ores

Sulfide ore samples used in this study were collected from Dongguashan Copper Mine in Anhui, China. Pyrite was purchased from Strem Chemical Co., Ltd., Boston, MA, USA. The collected sulfide ore and pyrite were dried in a vacuum at 80 °C for 24 h. The samples were crushed and sieved in the range of 96–120 μm before the experiments. An XRD (X-ray Diffractometer) is mainly used to measure powders or crystals, with the advantages of convenience and efficiency. In this paper, XRD was applied to analyze the composition of sulfide ore powders. The XRD (DY5261/Xpert3) machine was manufactured by CEM Corporation, USA. The scanning range of the experimental test was 5~90°, and the scanning interval was 5°/min. The XRD analysis results showed that the main components of sulfide ores included pyrite (FeS_2), $Fe_{0.91}S$, SiO_2, Fe_3O_4, and Fe_3S_4 (Figure 1). Further, a Scanning Electron Microscope (SEM) was utilized to take pictures of sulfide ores; it could be seen that the surface of the ore sample was comparatively flat and the surface of the large particle ore sample was attached with many small particles (Figure 2). The agglomeration effect of small particles may be induced by the high activity of the sulfide ores, which reduces their surface free energy [14]. The SEM (Quanta 250) was manufactured by FEI Company, Hillsboro, OR, USA. In addition, the elements contained in the sulfide ores were mainly Fe and S.

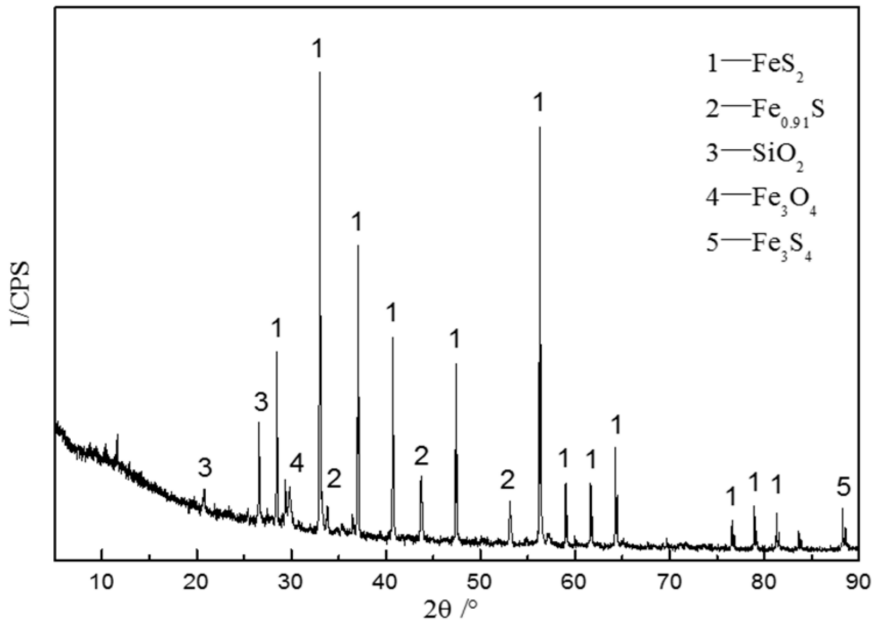

Figure 1. XRD spectra of the sulfide ores.

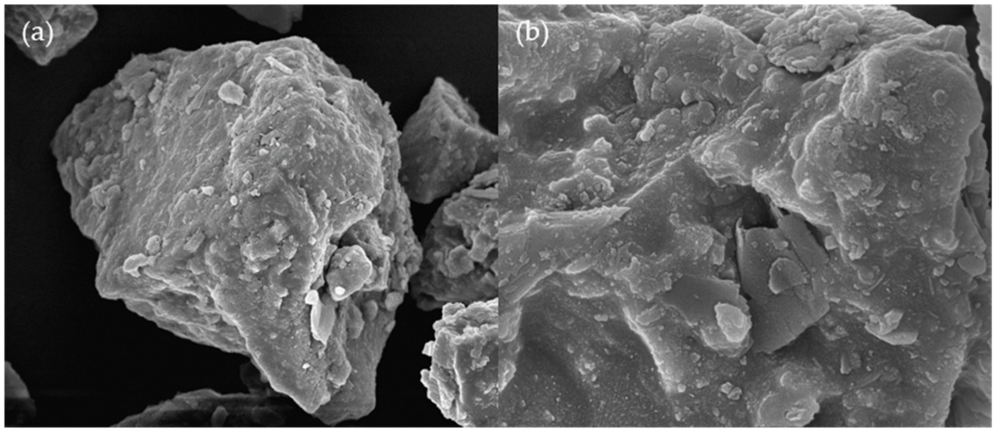

Figure 2. SEM images of sulfide ores: (**a**) 10 μm; (**b**) 3 μm.

2.2. Emulsion Explosive Matrix

Compositions of EE matrix are shown in Table 1. Ammonium nitrate, sodium nitrate, compound wax, and emulsifier are all industrial products. These products were sourced from chemical plants in China and had a purity of up to 99%. The emulsifier was a PIBSA derivative. The wax was a special compound wax for explosives, which was composed of oily waxes in different distillation ranges and a variety of additives. The weight of impurities was no more than 0.05%. The production process of EE matrix is illustrated in Figure 3. The procedure for EE matrix preparation included three steps. Firstly, ammonium nitrate, sodium nitrate, and water were mixed and heated up to 110 °C to make a water phase mixture. Secondly, the wax was mixed with an emulsifier at 90 °C to make the oil phase mixture. Thirdly, the water phase mixture and oil phase mixture were mixed under the speed of the emulsifying and dispersing machine at 1200 r/min, 90 °C for 2 min to make EE matrix. Finally, the powder of sulfide ores and pyrite samples were mixed with the emulsion explosive matrix and ammonium nitrate, respectively (Figure 4). Four kinds of samples were prepared, i.e., (a): 100% emulsion explosive matrix, (b): 50% sulfide ores and 50% emulsion explosive matrix, (c): 100% ammonium nitrate, (d): 50% pyrite and 50% ammonium nitrate.

Table 1. Compositions of emulsion explosive matrix.

Compositions	Ammonium Nitrate	Sodium Nitrate	Compound Wax	Water	Emulsifier
wt%	70	14	9	4	3

Note: Compound wax was composed of oil-containing wax of different distillation ranges and a variety of additives.

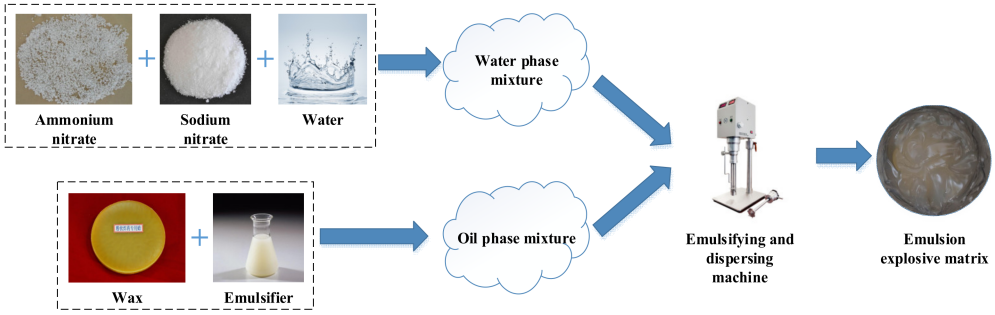

Figure 3. The production process of emulsion explosive matrix.

Figure 4. The experimental samples.

2.3. STA (Simultaneous Thermal Analyzer)

Thermal decomposition experiments were carried out by a STA analyzer (449C, NETZSCH, Selb, Germany), which has a mass resolution of 0.1 μg. Approximately 3.0 mg samples were placed in the alumina crucible to conduct a TG-DTG test. The samples were heated up from 25 °C to 350 °C with heating rates of 3, 5, 10 and 15 K/min under an air atmosphere. The airflow rate was 20 mL/min. To guarantee the accuracy of the experimental results, all the experiments were performed at least three times. The sample weight, airflow rate, reaction atmosphere, and heating rate were strictly regulated, and experiment error was less than 5%. In this paper, the average values of the repeated experimental results were regarded as the final testing results.

3. Results and Discussion

3.1. TG/DTG of Samples with Different Heating Rates

To investigate the influence of heating rate on the thermal decomposition of samples, TG-DTG analysis was also carried out on four samples at the heating rates of 3, 5, 10, and 15 K/min, separately. Figures 5 and 6 show the TG and DTG curves of four samples at different heating rates. According to TG curves and DTG curves, it can be concluded that the trend of curves is similar at different heating rates and shifts to higher temperatures with increasing heating rates.

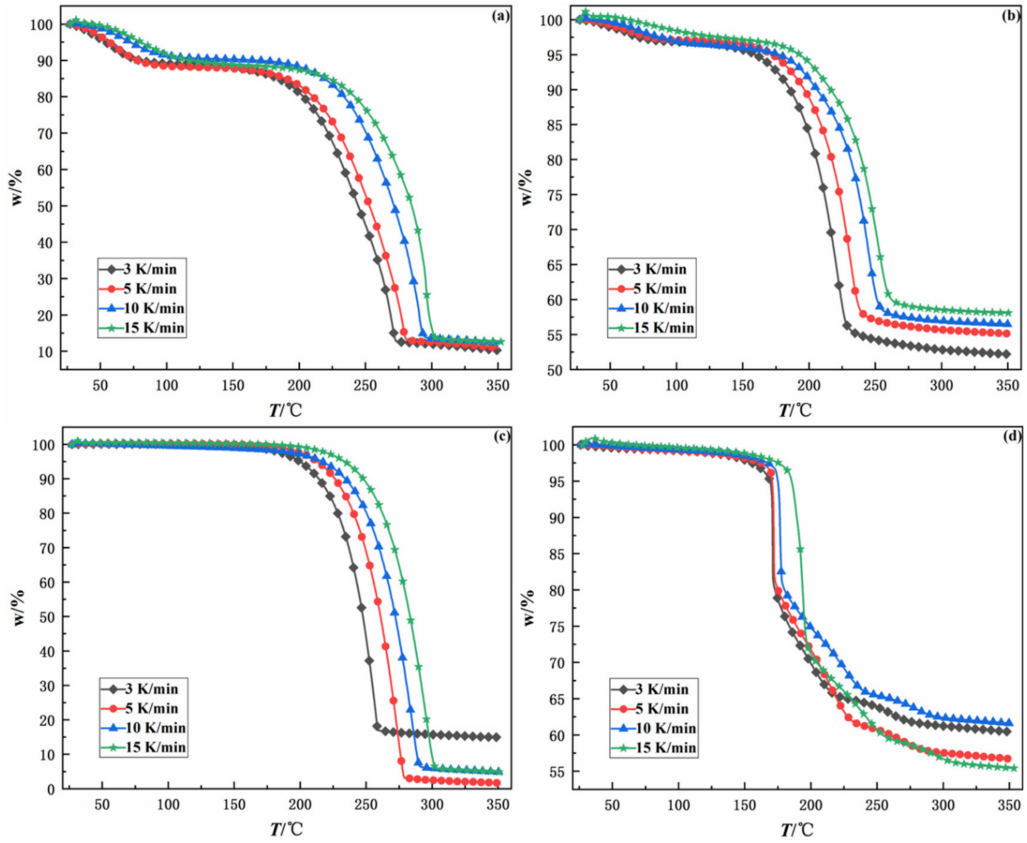

Figure 5. TG curves of four samples at different heating rates. (**a**): 100% emulsion explosive matrix, (**b**): 50% sulfide ores and 50% emulsion explosive matrix, (**c**): 100% ammonium nitrate, (**d**): 50% pyrite and 50% ammonium nitrate.

The characterization parameters of four samples at different heating rates are presented in Table 2, including ignition temperature (T_0), burnout temperature (T_f), and the maximum peak temperature (T_m). The ignition temperature is namely the temperature at which samples begin to burn. The burnout temperature is the temperature corresponding to 98% conversion on the TG curve. The maximum peak temperature is the temperature corresponding to the point where the chemical reaction intensity of the sample is largest; namely, the temperature corresponding to the valley point on the DTG curve. In general, the T_0, T_f and T_m of all four samples increased with heating rate owing to the thermal hysteresis effect [15,16]. It should be noted that the T_0, T_f and T_m of EE matrix and sulfide ores are lower than those of EE matrix. The maximum peak temperature and the burnout temperature of EE matrix and sulfide ores are about 45 °C lower than those of EE matrix. The ignition temperature of EE matrix and sulfide ores is 27.52–53.74 °C lower than that of EE matrix. The above results indicate that sulfide ores can significantly reduce the thermal stability of EE matrix, accelerate the thermal decomposition rate of EE matrix, and increase the risk of self-detonation of EE matrix.

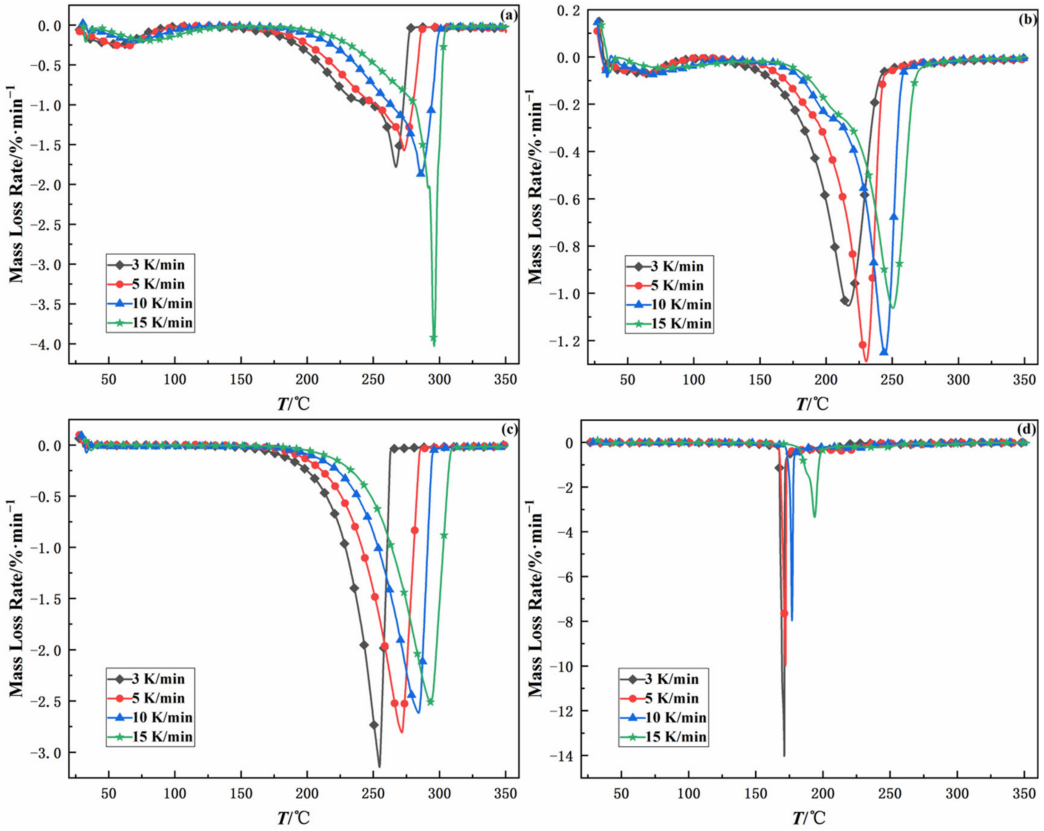

Figure 6. DTG curves of four samples at different heating rates. (**a**): 100% emulsion explosive matrix, (**b**): 50% sulfide ores and 50% emulsion explosive matrix, (**c**): 100% ammonium nitrate, (**d**): 50% pyrite and 50% ammonium nitrate.

Table 2. Characterization parameters of four samples with different heating rates.

	Heating Rate (K/min)	T_0 (°C)	T_f (°C)	T_m (°C)		Heating Rate (K/min)	T_0 (°C)	T_f (°C)	T_m (°C)
(a)	3	231.83	273.83	267.60	(c)	3	232.52	259.24	254.79
	5	234.91	282.96	273.57		5	245.19	278.67	271.86
	10	253.43	298.38	286.43		10	254.80	290.48	283.94
	15	281.33	305.95	296.28		15	264.79	301.41	292.32
(b)	3	193.99	230.16	217.13	(d)	3	170.76	274.21	170.85
	5	207.39	238.57	230.78		5	171.42	283.89	172.56
	10	222.65	252.43	244.50		10	175.41	292.25	177.03
	15	227.59	260.29	250.93		15	188.49	307.66	193.95

Note: (a): 100% emulsion explosive matrix, (b): 50% sulfide ores and 50% emulsion explosive matrix, (c): 100% ammonium nitrate, (d): 50% pyrite and 50% ammonium nitrate.

Compared with the ignition temperature of AN, the ignition temperature of AN and pyrite is reduced by 61.76–79.39 °C, and the maximum peak temperature of AN and pyrite is 83.94–106.91 °C lower than that of AN. It indicates that pyrite can significantly reduce the thermal stability of AN and increase the possibility of AN's spontaneous combustion [17]. Moreover, pyrite has a more significant influence on the thermal stability of AN than sulfide ores on the EE matrix.

Additionally, it can be concluded that the T_0, T_f and T_m of EE matrix are similar to those of AN, which shows that the thermal decomposition of EE matrix is mainly the thermal decomposition of AN [8].

3.2. Thermal Decomposition Behavior of Different Samples

Since TG-DTG curves of the samples followed the same trend at different heating rates, the heating rate of 10 K/min was taken as an example to analyze the thermal decomposition behavior of the samples (Figure 7). According to Figure 7, the masses of samples (a) and (b) underwent four processes: slight decrease, constant, dramatic decrease, and gradual stable, while the masses of samples (c) and (d) experienced three processes: constant, dramatic decrease, and gradual stable.

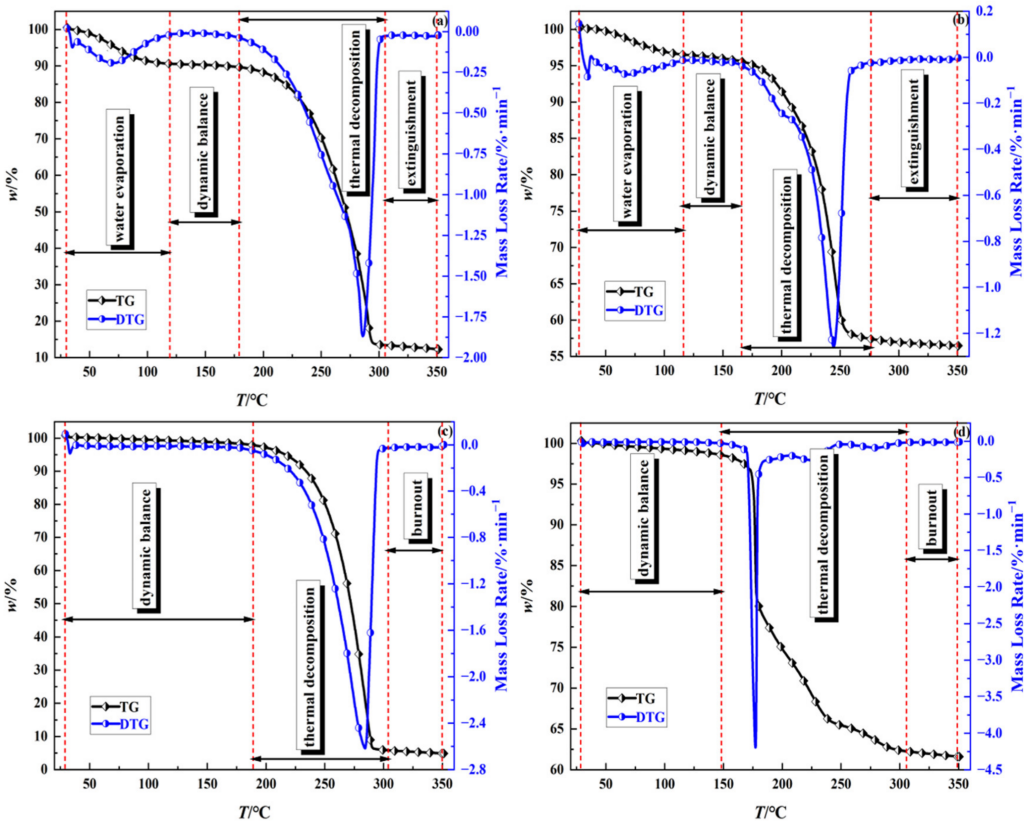

Figure 7. TG-DTG curves of thermal decomposition of four samples at 10 K/min: (**a**): 100% emulsion explosive matrix, (**b**): 50% sulfide ores and 50% emulsion explosive matrix, (**c**): 100% ammonium nitrate, (**d**): 50% pyrite and 50% ammonium nitrate.

Thermal decomposition processes of EE matrix, sulfide ores and EE matrix can be divided into water evaporation, dynamic balance, thermal decomposition, and extinguishment stages [18,19]. In the water evaporation stage, the droplet of emulsion appears first, causing the water to evaporate, resulting in slight mass loss of samples [8]. The mass loss of sample (a) was about 9%, which was the same as the water content in the EE matrix. The mass loss of sample (b) was about 2.5%, which was lower than the mass of water in the mixture. It may be responsible for the oxidation reaction among sulfide ores, water, and oxygen. The possible reaction equations are shown in Equations (1)–(4) [20,21]:

$$2FeS_2 + 7O_2 + 2H_2O = 2FeSO_4 + 2H_2SO_4 \quad (1)$$

$$4FeS_2 + 15O_2 + 14H_2O = 4Fe(OH)_3 + 8H_2SO_4 \quad (2)$$

$$4FeS_2 + 15O_2 + 8H_2O = 2Fe_2O_3 + 8H_2SO_4 \quad (3)$$

$$4Fe_3O_4 + O_2 = 6Fe_2O_3 \quad (4)$$

Subsequently, since the temperature for thermal decomposition of EE matrix was not reached, the masses of samples (a) and (b) kept constant. With the increase in temperature, rapid mass losses of samples (a) and (b) occurred at the temperatures 180–304 °C and

165–270 °C, respectively. This mainly resulted from the thermal decomposition of EE matrix and the reaction between sulfide ores and EE matrix [8,11]. The possible reaction equations are given as follows [8,22]:

$$NH_4NO_3 = NH_3 + HNO_3 \quad (5)$$

$$NH_4NO_3 = N_2O + 2H_2O \quad (6)$$

$$14FeS_2 + 91NH_4NO_3 = 52NO + 26SO_2 + 6Fe_2O_3 + 78NH_3 + 26N_2O + 2FeSO_4 + 65H_2O \quad (7)$$

In the final stage of the reaction, the mass of sample (a) was approximately 12.5% of the initial mass; sample (b) was reduced to 57.5% of the initial mass. Both sample (a) and sample (b) had three mass loss peaks. The temperatures of the first and second mass loss peaks were lower than 100 °C, corresponding to water evaporation in the first stage of the reaction. Besides, the temperature at the maximum mass loss peak of sample (a) was about 285 °C, and that of sample (b) was about 244 °C. The burnout temperature of sample (a) was approximately 300 °C, and that of sample (b) was approximately 250 °C. Moreover, it can be inferred that the presence of sulfide ores accelerated the decomposition rate of the EE matrix [8].

The whole reaction process of AN can be subdivided into the dynamic balance stage, thermal decomposition stage, and burnout stage [17,23,24]. The overall reaction trend of the mixture of AN and pyrite was similar. In the dynamic balance stage, AN had excellent thermal stability and the overall quality remained constant. In the thermal decomposition stage, huge mass losses occurred on samples, owing to the thermal decomposition of AN and the reaction between pyrite and AN. The possible chemical reactions are presented in Equations (4)–(6). In the end, the mass loss of sample (c) was about 97% and the mass loss of sample (d) was about 37.5%. Consequently, it can be derived that most of the mass of AN reacted entirely. Moreover, the thermal decomposition temperature of sample (c) was approximately 190 °C, while that of sample (d) was approximately 160 °C. This can be attributed to the presence of pyrite, which reduced the decomposition temperature of AN [5,8,22].

3.3. Thermal Oxidative Decomposition Kinetics Analysis

Integral and differential methods are usually adopted to calculate apparent activation energy [25,26]. Besides, the calculation error of the integral methods is more minor. The Coats–Redfern method is the most commonly used non-isothermal reaction mechanism function, which is categorized as an integral method and can fully consider the influence of the reaction mechanism on the calculation results [27]. In this study, the Coats–Redfern method was applied to determine the activation energy of the four samples at different heating rates.

According to the chemical reaction kinetics, the oxidative spontaneous combustion reactions of sulfide ores and EE matrix, pyrite and AN are gas-solid reactions; the reaction rate can be expressed by the Arrhenius law:

$$\frac{d\alpha}{dt} = Aexp\left(-\frac{E}{RT}\right)f(\alpha) \quad (8)$$

$$\alpha = \frac{m_0 - m_t}{m_0 - m_\infty} \quad (9)$$

where α is the conversion rate of oxidation decomposition of four samples, m_0 is the initial mass of the sample (g), m_t is the mass of the sample at time t (g), m_∞ is the mass of the sample at the end of the reaction (g), $f(\alpha)$ is the differential form of the reaction mechanism function, t is the reaction time, T is the reaction temperature (K), A is the pre-exponential

factor (s^{-1}), R is the molar gas constant (8.314 J/mol·K), E represents apparent activation energy of the reaction (kJ/mol).

$$\beta = \frac{dT}{dt} \tag{10}$$

where β is the heating rate (K/min). Equation (11) can be obtained by combining Equations (8) and (10).

$$\frac{d\alpha}{f(\alpha)} = \frac{A}{\beta} \exp\left(-\frac{E}{RT}\right) dT \tag{11}$$

According to the thermal analysis kinetics, the Coats–Redfern equation can be presented as follows:

$$\ln\left[\frac{G(\alpha)}{T^2}\right] = \ln\left[\frac{AR}{E\beta}\left(1 - \frac{2RT}{E}\right)\right] - \frac{E}{RT} \tag{12}$$

where $G(\alpha)$ represents the integral form of reaction mechanism function, different reaction mechanisms have their corresponding different forms. By substituting various reaction mechanism modes into Equation (12) and processing TG data to get the correlation coefficient R^2. The kinetic model with the best linear correlation represents the reaction mechanism of the thermal oxidation decomposition of samples. The integral form of reaction mechanism function is $G(\alpha) = \alpha + (1-\alpha)\ln(1-\alpha)$. In general, $\frac{E}{RT} \gg 1$, then $\left(1 - \frac{2RT}{E}\right)$ is approximately equal to 1. By plotting $\ln[G(\alpha)/T^2]$ to $1/T$, the fitting lines of samples can be obtained, as displayed in Figure 8. The apparent activation energy of the reaction could be derived from the corresponding slope.

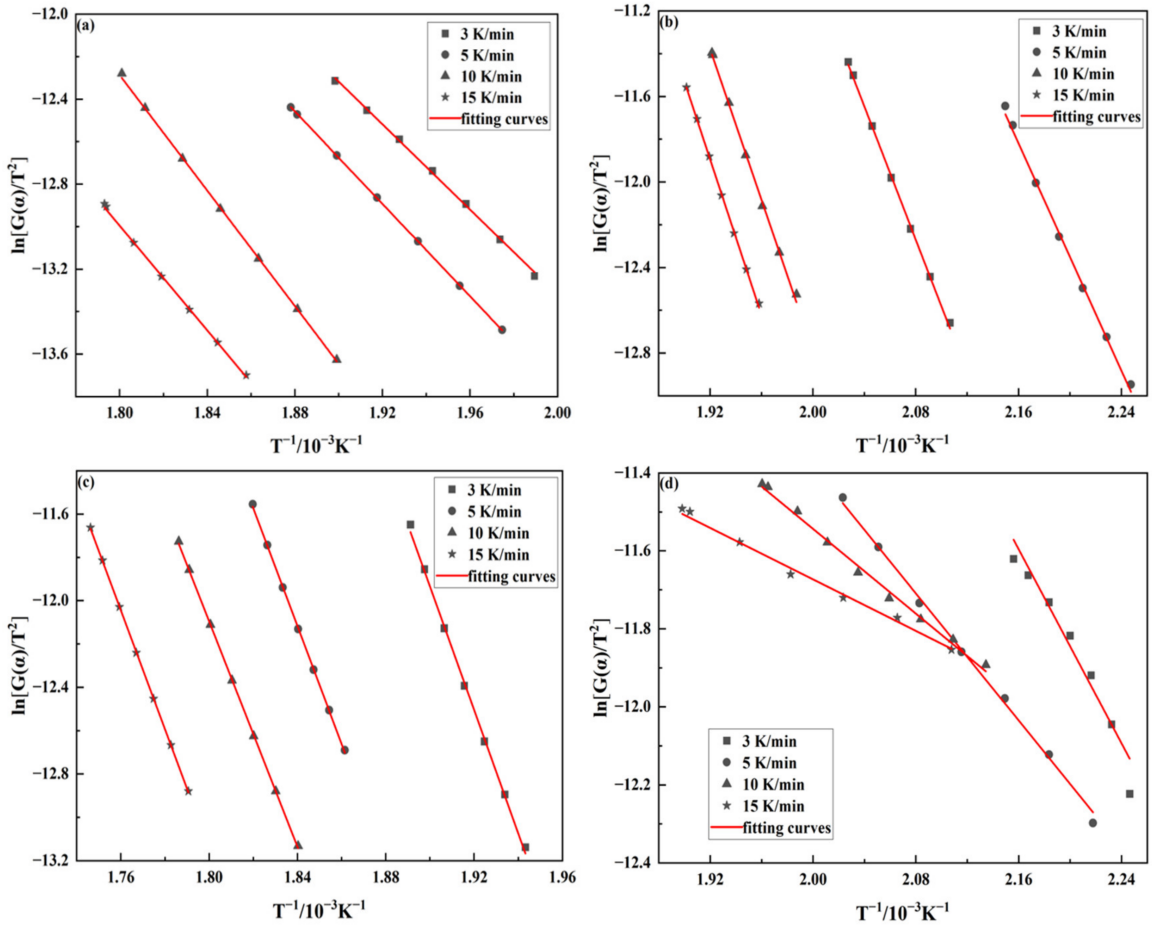

Figure 8. Fitting curves of four samples at different heating rates by Coats–Redfern method (**a**): 100% emulsion explosive matrix, (**b**): 50% sulfide ores and 50% emulsion explosive matrix, (**c**): 100% ammonium nitrate, (**d**): 50% pyrite and 50% ammonium nitrate.

As illustrated in Table 3, the activation energies of EE matrix with sulfide ores at different heating rates are lower than those of EE matrix. EE matrix's apparent activation energy at different heating rates is 83.44–112.9 kJ/mol, while that of EE matrix with sulfide ores is 47.32–66.64 kJ/mol. The above results indicate that sulfide ores have a catalytic effect on the thermal decomposition reaction of EE matrix. Besides, EE matrix with sulfide ores is more prone to spontaneous combustion and self-detonation. The activation energy of AN with pyrite at different heating rates is likewise much lower than that of AN. The apparent activation energy of AN at different heating rates is 216.2–228.2 kJ/mol, while that of pyrite with AN is 13.72–51.70 kJ/mol. This shows that pyrite has a catalytic effect on the thermal decomposition reaction of AN [11]. Furthermore, the activation energy of sample (d) varies wildly at different heating rates; this may be attributed to the thermal hysteresis/inertia effect caused by the use of various heating rates.

Table 3. Kinetic parameters of four samples at different heating rates by Coats–Redfern method.

	***Ea*, kJ/mol**				***R*²**			
	3 K/min	**5 K/min**	**10 K/min**	**15 K/min**	**3 K/min**	**5 K/min**	**10 K/min**	**15 K/min**
(a)	83.44	90.42	112.9	102.4	0.99891	0.99995	0.99984	0.99953
(b)	55.48	47.32	64.14	66.64	0.99914	0.99804	0.99833	0.99950
(c)	237.0	226.0	216.2	228.2	0.99892	0.99966	0.99989	0.99993
(d)	51.70	33.84	22.59	13.72	0.97123	0.99790	0.99118	0.98887

4. Conclusions

The thermal reaction kinetic characteristics of EE matrix and sulfide ores were investigated by employing thermal analysis techniques. In the presence of sulfide ores, the apparent activation energy of EE matrix decreased by 28.96–48.76 kJ/mol at different heating rates. The ignition temperature of EE matrix and sulfide ores was 27.52–53.74 °C lower than that of EE matrix, and the maximum peak temperature and the burnout temperature of EE matrix and sulfide ores were about 45 °C lower than those of EE matrix. It was observed that sulfide ores can significantly reduce the thermal stability of EE matrix and increase the risk of self-detonation of EE matrix. The presence of sulfide ores reduces the thermal decomposition temperature of EE matrix and accelerates the rate of decomposition of EE matrix. Moreover, in the presence of pyrite, the apparent activation energy of AN dropped by 185.3–214.48 kJ/mol at different heating rates. Moreover, the ignition temperature of AN and pyrite decreased by 61.76–79.39 °C. Therefore, pyrite reduces the thermal stability of AN and increases the risk of self-detonation of AN. Sulfide ores have a catalytic effect on the thermal decomposition of EE matrix, and pyrite has a catalytic effect on the thermal decomposition of AN. The reaction between sulfide ores and EE matrix is similar to the reaction between pyrite and AN. Compared with the impact of sulfide ores on the thermal decomposition characteristics of EE matrix, pyrite has a more significant effect on the thermal stability and activation energy of AN.

Author Contributions: Conceptualization, Y.H.; Data curation, Y.G. and Y.L.; Formal analysis, F.Y., Y.G., Y.H. and S.Y.; Funding acquisition, F.Y.; Investigation, Y.G., Y.L. and S.Y.; Methodology, F.Y., Y.G., Y.H. and S.Y.; Project administration, Y.H.; Supervision, F.Y. and Y.H.; Visualization, Y.L.; Writing—original draft, F.Y., Y.G. and Y.L.; Writing—review & editing, F.Y., Y.H. and S.Y. All authors have read and agreed to the published version of the manuscript.

Funding: This research was funded by the National Natural Science Foundation of China (51874100).

Institutional Review Board Statement: Not applicable.

Informed Consent Statement: Not applicable.

Conflicts of Interest: The authors declare that we do not have any commercial or associative interest that represents a conflict of interest in connection with the work submitted.

References

1. Cao, Y.; Tang, Y.; Yao, M.; Shang, P.; Zou, Z.; Qiu, G.; Xiong, X. Geological characteristics and resource potential of sulfur deposits in China. *Earth Sci. Front.* **2018**, *25*, 179–195.
2. Gu, D.; Zhou, K. Development theme of the modern metal mining. *Metal Mine.* **2012**, *41*, 1.
3. Steis, T.; Evans, W. Sulfide ore explosives exothermic reactions. *Cim Bull.* **1995**, *88*, 54–57.
4. Pan, W.; Jin, H.; Liu, Z.; Tang, J.; Cheng, S. Experimental and theoretical study on strengthening leaching of sulfide ores by surfactants. *Process Saf. Environ. Protect.* **2020**, *137*, 289–299. [CrossRef]
5. Gunawan, R.; Freij, S.; Zhang, D.K.; Beach, F.; Littlefair, M. A mechanistic study into the reactions of ammonium nitrate with pyrite. *Chem. Eng. Sci.* **2006**, *61*, 5781–5790. [CrossRef]
6. Priyananda, P.; Djerdjev, A.M.; Gore, J.; Neto, C.; Beattie, J.K.; Hawkett, B.S. Premature detonation of an NH_4NO_3 emulsion in reactive ground. *J. Hazard. Mater.* **2015**, *283*, 314–320. [CrossRef]
7. Nakmura, H.; Iwasaki, M.; Sato, S.; Hara, Y. The reaction of ammonium nitrate with pyrite. *J. Hazard. Mater.* **1994**, *36*, 293–303. [CrossRef]
8. Xu, Z.; Wang, Q.; Fu, X. Thermal stability and mechanism of decomposition of emulsion explosives in the presence of pyrite. *J. Hazard. Mater.* **2015**, *300*, 702–710. [CrossRef]
9. Liu, F.; Zhu, S.; Xing, H.; Zhang, H. Comparison of Thermal Decomposition Characteristics of Emulsion Explosives in Two Atmospheres. *Initiat. Pyrotech.* **2018**, *4*, 40–44.
10. Djerdjev, A.M.; Priyananda, P.; Gore, J.; Beattie, J.K.; Neto, C.; Hawkett, B.S. The mechanism of the spontaneous detonation of ammonium nitrate in reactive grounds. *J. Environ. Chem. Eng.* **2018**, *6*, 281–288. [CrossRef]
11. Vázquez, M.; Moreno-Ventas, I.; Raposo, I.; Palma, A.; Díaz, M.J. Kinetic of pyrite thermal degradation under oxidative environment. *J. Therm. Anal. Calorim.* **2020**, *141*, 1157–1163. [CrossRef]
12. Ruan, S.; Wang, C.; Jie, X.; Yin, F.; Zhang, Y.; Yao, Z.; Chen, Y. Kinetics of pyrite multi-step thermal decomposition in refractory gold sulphide concentrates. *J. Therm. Anal. Calorim.* **2022**, *147*, 3689–3702. [CrossRef]
13. Yang, F.; Wu, C.; Li, Z. Spontaneous combustion tendency of fresh and pre-oxidized sulfide ores. *J. Cent. South Univ.* **2014**, *21*, 715–719. [CrossRef]
14. Liu, H.; Xiang, C.L.; Hong, R.; Song, Y.; Jin, K.; Zhu, K.; Yang, C.; Lv, C. Thermal behavior and kinetics of sulfide concentrates. *Therm. Sci.* **2019**, *23*, 2801–2811. [CrossRef]
15. Lopes, F.C.R.; Tannous, K. Coconut fiber pyrolysis: Specific heat capacity and enthalpy of reaction through thermogravimetry and differential scanning calorimetry. *Thermochim. Acta* **2022**, *707*, 179087. [CrossRef]
16. Xiao, Y.; Zhang, H.; Liu, K.H.; Shu, C.M. Macrocharacteristics and the inhibiting effect of coal spontaneous combustion with various treatment durations of ionic liquids. *Thermochim. Acta* **2021**, *703*, 179012. [CrossRef]
17. Chanturvedi, S.; Dave, P.N. Review on Thermal Decomposition of Ammonium Nitrate. *J. Energ. Mater.* **2013**, *31*, 1–26. [CrossRef]
18. Xiang, C.; Liu, H.; Mu, J.; Lang, Z.; Wang, H.; Nie, R.; Kong, F. Thermodynamic model and kinetic compensation effect of spontaneous combustion of sulfur concentrates. *ACS Omega* **2020**, *5*, 20618–20629. [CrossRef]
19. Li, X.; Shang, Y.; Chen, Z.; Chen, X.; Niu, F.; Yang, M.; Zhang, Y. Study of spontaneous combustion mechanism and heat stability of sulfide minerals powder based on thermal analysis. *Powder Technol.* **2017**, *309*, 68–73. [CrossRef]
20. Wu, C.; Meng, T. Experimental investigation on chemical thermodynamic behavior of sulfide ores during spontaneous combustion. *West-China Explor. Eng.* **1995**, *7*, 57–65.
21. Gu, D.; Li, X. *Modern Mining Science and Technology for Metal Mineral Resources*; China Metallurgical Industry Press: Beijing, China, 2006.
22. Gunawan, R.; Zhang, D. Thermal stability and kinetics of decomposition of ammonium nitrate in the presence of pyrite. *J. Hazard. Mater.* **2009**, *165*, 751–758. [CrossRef] [PubMed]
23. Fujisato, K.; Habu, H.; Miyake, A.; Hori, K. Thermal decomposition of ammonium nitrate modeling of thermal dissociation in thermal analysis. *Sci. Technol. Energ. Mater.* **2014**, *75*, 28–36.
24. Babrauskas, V.; Leggtet, D. Thermal decomposition of ammonium nitrate. *Fire Mater.* **2020**, *44*, 250–268. [CrossRef]
25. Gupta, G.K.; Mondal, M.K. Kinetics and thermodynamic analysis of maize cob pyrolysis for its bioenergy potential using thermogravimetric analyzer. *J. Therm. Anal. Calorim.* **2019**, *137*, 1431–1441. [CrossRef]
26. Jayapal, S.N.M.; Dubey, V.K.; Dinesh, S.; Wahab, A.; Khaleel, A.A.; Kadiresh, P.N. Thermal stability and kinetic study of blended Beeswax-ethylene vinyl acetate based hybrid rocket fuels. *Thermochim. Acta* **2021**, *702*, 178989. [CrossRef]
27. Li, X.; Wu, T.; Zhou, Q.; Peng, Z.; Liu, G. Kinetics of oxidation roasting of molybdenite with different particle sizes. *Trans. Nonferrous Met. Soc. China* **2021**, *31*, 842–852. [CrossRef]